ACS Medicinal Chemistry Letters

Letter

pubs.acs.org/acsmedchemlett

Discovery of Spiro[cyclohexane-dihydropyrano[3,4-*b*]indole]-amines as Potent NOP and Opioid Receptor Agonists

Stefan Schunk,*[,†] Klaus Linz,[‡] Sven Frormann,[†] Claudia Hinze,[†] Stefan Oberbörsch,[†] Bernd Sundermann,[†] Saskia Zemolka,[†] Werner Englberger,[§] Tieno Germann,[§] Thomas Christoph,[∥] Babette-Y. Kögel,[∥] Wolfgang Schröder,[∥] Stephanie Harlfinger,[⊥] Derek Saunders,[⊥] Achim Kless,[#] Hans Schick,[○] and Helmut Sonnenschein[○]

[†]Departments of Medicinal Chemistry, [‡]Preclinical Drug Safety, [§]Molecular Pharmacology, [∥]Pain Pharmacology, [⊥]Pharmacokinetics, and [#]Discovery Informatics, Global Drug Discovery, Grünenthal Innovation, Grünenthal GmbH, D-52099 Aachen, Germany

[○]ASCA GmbH Angewandte Synthesechemie Adlershof, Magnusstr. 11, 12489 Berlin, Germany

Supporting Information

ABSTRACT: We report the discovery of spiro[cyclohexane-pyrano[3,4-*b*]indole]-amines, as functional nociceptin/orphanin FQ peptide (NOP) and opioid receptor agonists with strong efficacy in preclinical models of acute and neuropathic pain. Utilizing 4-(dimethylamino)-4-phenylcyclo-hexanone **1** and tryptophol in an oxa-Pictet−Spengler reaction led to the formation of spiroether **2**, representing a novel NOP and opioid peptide receptor agonistic chemotype. This finding initially stems from the systematic derivatization of **1**, which resulted in alcohols **3**−**5**, ethers **6** and **7**, amines **8**−**10**, **22**−**24**, and **26**−**28**, amides **11** and **25**, and urea **12**, many with low nanomolar binding affinities at the NOP and mu opioid peptide (MOP) receptors.

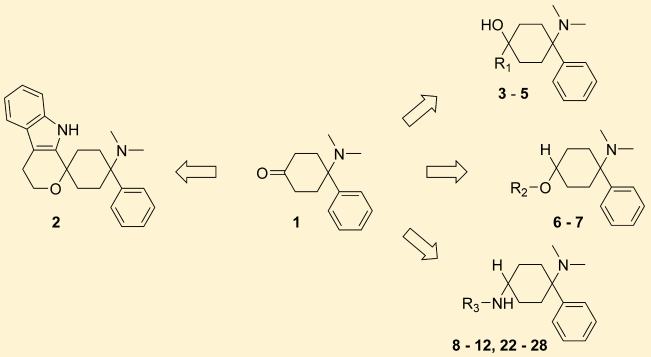

KEYWORDS: *NOP receptor agonist, MOP receptor agonist*

For decades, opioid peptide receptors have been targeted for the treatment of pain, and the present day opioids remain the most effective clinically used drugs for the treatment of moderate to severe acute and chronic pain. However, opioids also carry the risk of severe side effects such as respiratory depression, nausea, vomiting, and constipation, and their use may lead to physical dependence and tolerance.[1] The nociceptin receptor and its endogenous ligand nociceptin/orphanin FQ (N/OFQ), a 17-amino acid neuropeptide, have been described almost 20 years ago.[2,3] Because of its partial homology to the three opioid peptide receptor subtypes mu opioid peptide (MOP), kappa opioid peptide (KOP), and delta opioid peptide (DOP) and its insensitivity to opioid agonists (e.g., morphine) and antagonists (e.g., naloxone), the receptor was initially termed "opioid-receptor-like 1" (ORL 1). More recently, however, it was renamed after its endogenous ligand to nociceptin/orphanin FQ peptide (NOP) receptor. Despite its structural and functional homology to opioid receptors, the NOP receptor is not an opioid peptide receptor from a pharmacological perspective and, as such, is considered a nonopioid member of the opioid peptide receptor family.[4]

NOP and MOP receptor agonists modulate pain and nociception via distinct yet related targets. Addressing both mechanisms may constitute a novel approach for the development of innovative analgesics. Indeed, recent publications indicate that concurrent activation of NOP and MOP receptors may potentiate opiate analgesia and at the same time lead to an improved side effect profile.[5,6] We therefore aimed at identifying highly potent, small molecule NOP and MOP receptor agonists.

This endeavor started with a literature-to-lead approach based on cyclohexanone **1**, which has previously been reported by Lednicer et al. as representing a novel class of analgesics.[7,8] As a starting point it was clear that, due to its size, compound **1** would lack key interactions within the binding pocket of both the NOP and MOP receptors and therefore would have only minimal receptor binding affinities (K_i(NOP) = 1.5 μM; K_i(MOP) = 1.7 μM). It was our strategy to utilize **1** as a core and its ketone moiety for functionalization. Thus, fixing the 4-*N*,*N*-dimethylamino-4-phenyl-cyclohexane head, we initiated a scouting exercise probing a range of simple aryl and more complex moieties.

The impact of the linking functionality and linker length on the NOP and MOP receptor binding affinities was to be investigated first. Alcohols **3a**−**5a**, ethers **6a**,**b** and **7a**, amines

Received: March 19, 2014
Accepted: June 12, 2014
Published: June 24, 2014

   dx.doi.org/10.1021/ml500116x | *ACS Med. Chem. Lett.* 2014, 5, 851−856

Scheme 1. Synthesis of Investigated Chemotypes[a]

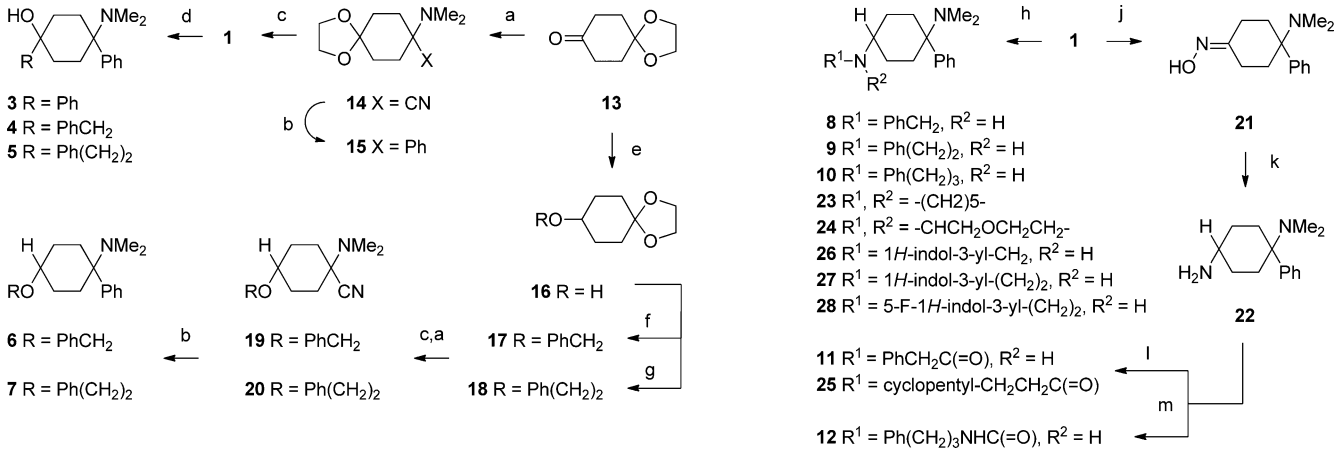

[a]Reagents and conditions: (a) (i) $HNMe_2/H_2O$, MeOH, $HNMe_2$·HCl, KCN, 67−99%; (b) (i) PhMgCl, THF, 0 °C to rt; (ii) NH_4Cl, H_2O, 0 °C to rt; (iii) HCl, Et_2O; (iv) 25% NH_3 aq. pH 8−9, 28−92%; (c) (i) HCl aq.; (ii) NaOH aq., 66−99%; (d) (i) RMgHal, THF; (ii) phosphate buffer, pH 7, 13−30%; (e) $NaBH_4$, ethanol, 0 °C, 98%; (f) (i) KO*t*-Bu, DMF; (ii) BnCl; (iii) H_2O, 0 °C; (iv) distillation, 77%; (g) (i) $Ph(CH_2)_2I$, AgOTf, anh MeCN, reflux; (ii) $NaHCO_3$, EtOAc, 12%; (h) R^1R^2NH, $NaBH(OAc)_3$, DCE, THF, 7−45%; (j) H_2NOH·HCl, Amberlyst A 21, quantitative yield; (k) Devarda (Cu/Zn/Al) alloy, MeOH, 5 N NaOH, 97%; (l) RCOCl, Et_2O, (70−71%); (m) $Ph(CH_2)_3NHCOOPh$, 1,4-dioxane, reflux; 53%.

8a−10a, amide **11a**, and urea **12a** were scrutinized as linking moieties.

Essentially, all examples in this article are based on 4-dimethyl-4-phenyl-cyclohexanone **1** (Scheme 1), which was prepared from monoketal-protected 1,4-cyclohexanedione **13**. Utilizing this in a Strecker synthesis gave aminonitrile **14**, which, when employed in a Bruylants reaction, furnished the ketal-protected phenyl dimethylamino-cyclohexane **15**. Ketal deprotection gave **1**.

Tertiary alcohols **3−5** were obtained by addition of Grignard reagents to **1**.[9] Ethers **6** and **7** were obtained in a 5 step sequence starting from the monoketal-protected 1,4-diketone **13**. Reduction of the ketone to the secondary alcohol **16** and subsequent alkylation gave ethers **17** and **18**, which were deprotected, converted into dimethylamino-nitriles **19** and **20**, and subjected to the Bruylants reaction to yield diastereomeric mixtures of ethers **6** and **7**. Amines were prepared by reductive amination of cyclohexanone **1** with primary or secondary amines to yield cyclohexyl-1,4-diamines **8** to **10**. Amides were prepared by reducing cyclohexanone oxime **21** to the corresponding primary amine **22**, which was subsequently converted into amide **11a** and urea **12a**.

The tertiary alcohols **3a−5a** allowed us to assess the impact of the spacer length, between the cyclohexyl core and the new aryl moiety, on the NOP and MOP receptor binding affinities. Phenyl and benzyl compounds **3a** and **4a**, representing a C_0 and C_1 carbon spacer, showed only moderate binding activities at the NOP receptor. Extending the carbon spacer by one further carbon atom (C_2 spacer), exemplified by phenethyl example **5a**, resulted in single digit nanomolar potencies. Furthermore, crucially with **5a** we had identified a compound that demonstrated equal binding affinities for the NOP and MOP receptors.

The potency shift induced by the extended spacer could be rationalized through docking studies. Compounds with a prolonged spacer are able to reach deeper into the lipophilic pocket of the binding site and form additional hydrophobic interactions with residues Ile127, Val126, and Trp116 (see Figure 1).

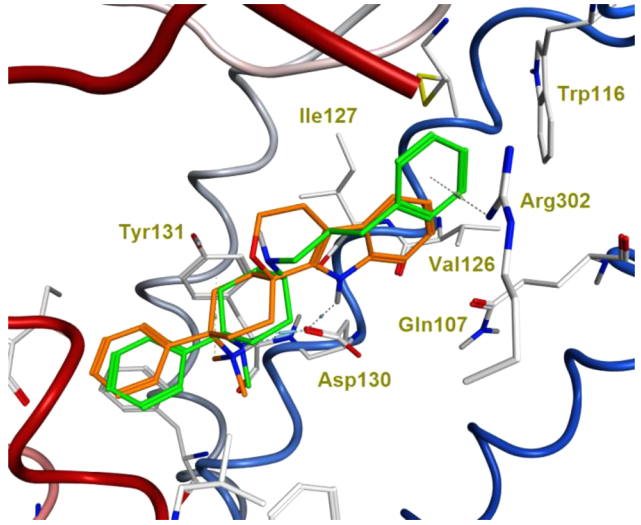

Figure 1. Binding mode of **2a**/**10a** in the NOP receptor.

Ether linkers were also well tolerated (**6a** and **7a**) resulting in double digit nanomolar potencies for **6a**. Interestingly, **6a** and **7a** were significantly more potent at the MOP receptor than at the NOP receptor, and the trans diastereomer **6a** demonstrated superior potency on both receptors over the cis diastereomer **6b**. Amine linkage was also well tolerated, as exemplified by examples **8a** to **10a**. The dibasic analogue **8a** led to a leap in binding potency at the NOP receptor, as compared to ether **6a**, being equipotent to the corresponding alcohol **5a**.

One could presume that hydrogen bond donation enables an additional interaction with the receptor, especially since carboxamide **11a** and urea **12a** also showed single digit nanomolar potencies.

Docking studies strengthened this hypothesis revealing potential interactions with Tyr131 or Gln107 (see Figure 1). In analogy to the alcohol series, the binding potencies within the amine series increased with the spacer length as in **9a** and **10a**.

dx.doi.org/10.1021/ml500116x | *ACS Med. Chem. Lett.* 2014, 5, 851−856

Table 1. Alcohol, Ether, and Amine Linkers

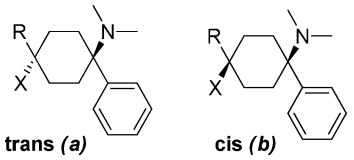

compd	X	R	config	% inhibition @ 1 μM or K_i (nM) *h*NOPr	*h*MOPr
3a	Ph	OH	trans	205	44.5
4a[a]	$PhCH_2$	OH	trans	1600	62.5%
5a[a]	$Ph(CH_2)_2$	OH	trans	4.4	1.9
6a[a]	$PhCH_2O$	H	trans	78	12
6b[a]	$PhCH_2O$	H	cis	290	830
7a	$Ph(CH_2)_2O$	H	trans[c]	81.5%	98.5%
8a[b]	$PhCH_2NH$	H	trans	10	3
9a[b]	$Ph(CH_2)_2NH$	H	trans	7.4	11
10a[b]	$Ph(CH_2)_3NH$	H	trans	0.5	22
11a[a]	$PhCH_2$–C(=O)NH	H	trans[d]	5.4	2.1
12a[a]	$Ph(CH_2)_3$–NHC(=O)NH	H	trans	1.9	0.7

[a]Hydrochloride. [b]Dihydrochloride. [c]Trans/cis mixture (5:3). [d]Trans/cis mixture (2:1).

The incorporation of a simple aryl moiety has already resulted in a significant increase of the receptor binding potencies as compared to **1** (Table 1), which was in accordance with previous findings by Lednicer et al.[11] Key learnings, which were to be considered while further optimizing the compounds, were the beneficial impact of H-bond donors and the spacer length on the receptor binding affinities as well as the significant impact of the stereochemistry.

For most examples, both diastereomers were isolated from the mixture via column chromatography. Relative configuration of key compounds was assigned by 2D homonuclear NOESY NMR measurements.

In a second round we set out to apply our key learnings and explore our options to modify the phenyl moiety itself (see Table 2). Complete removal of the aryl residue, as exemplified in diamine **22**, resulted only in weak activities at the NOP and especially MOP receptors. Nonaromatic replacements, exemplified by 1-piperidinyl **23** or 4-morpholinyl **24** again did not achieve the desired low nanomolar potencies. Moreover, potent NOP and MOP receptor binding only returned upon linking a long aliphatic side chain via an amide group **25**.

Probing both the role of a lipophilic pendant and the potential for identifying further beneficial H-bond donor receptor interactions triggered the use of indoles and the synthesis of examples **26** to **28**. The free NH indole derivative **26a** exhibited good levels of potency at the NOP and MOP receptors (see Table 2). Increasing the spacer length from one carbon atom to two **27a** gave an example with high binding affinities at the NOP and MOP receptors.

Following the observation from compound **27a** that highly potent NOP receptor binding can be achieved, albeit at the loss of MOP receptor affinities, it was reasoned that it may be possible to regain MOP receptor potency through replacing the amino linker with the ether linkage as exemplified by *h*MOPr biased (×6.5) compound **6a**. We therefore set out to synthesize compound **29** (Scheme 2).

We envisioned a reductive etherification of ketone **1** with the trimethylsilyl ether of tryptophol **30** under TMSOTf catalysis.[10] To our disappointment we did not obtain the desired product **21**, but instead isolated spiroethers **2a** and **2b**. These products resulted from a cyclization that had been known for quite some

Table 2. Amine and Amide Linked Examples

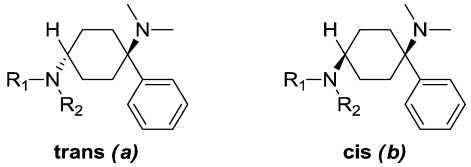

compd	R_1	R_2	config	% inhibition @ 1 μM or K_i (nM) *h*NOPr	*h*MOPr
22a	H	H	trans	120	69%
23b[a]	$-(CH_2)_5-$		cis	110	56%
24b[a]	$-CH_2CH_2OCH_2CH_2-$		cis	810	40%
25a[a]	cyclopentyl$(CH_2)_2$C(=O)	H	trans	0.5	0.3
26a	1*H*-indol-3-yl-CH_2	H	trans[c]	5.4	6.4
27a[b]	1*H*-indol-3-yl-$(CH_2)_2$	H	trans	1.1	9.5
28a[b]	5-F-1*H*-indol-3-yl-$(CH_2)_2$	H	trans	0.4	9

[a]Hydrochloride. [b]Dihydrochloride. [c]Trans/cis mixture (85:15).

Scheme 2. Spirocyclization of Tryptophol and Analogues with 1

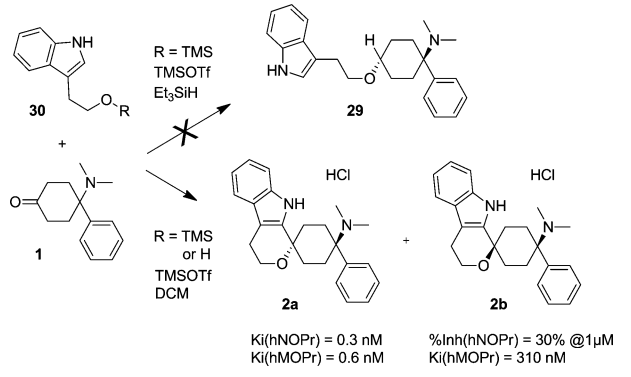

dx.doi.org/10.1021/ml500116x | ACS Med. Chem. Lett. 2014, 5, 851−856

time and has recently been coined oxa-Pictet−Spengler reaction.[12]

The trans diastereomer **2a** hydrochloride exhibited very high binding affinities to the NOP as well as the MOP receptors K_i(*h*NOPr) = 0.3 nM (N = 4, SEM = 0.05 nM), K_i(*h*MOPr) = 0.6 nM (N = 2, SEM = 0.14 nM), while the cis-diastereomer **2b** was significantly less active (%Inh.(*h*NOPr) = 30% @1 μM, K_i(*h*MOPr) = 310 nM). This observation is in line with the deterioration in binding affinity observed previously in the uncyclized series (**6a** vs **6b**) and could be retrospectively explained by docking studies. More detailed characterization revealed that **2a** hydrochloride had binding affinities of 4.9 nM (N = 3, SEM = 0.8 nM) and 2.3 nM (N = 3, SEM = 0.63 nM) at the hDOP and hKOP receptors.

Examples showed a stepwise binding affinity increase upon side chain prolongation. The binding mode of elongated compound **10a** (green) is shown as compared to **2a** (orange). It occupies the free space on the right side formed by trans membrane helixes 7 (hidden for clarity) and 1 and 2 (blue trans membrane helixes). The interactions within that pocket are determined by hydrophobic residues and additional cation−pi interactions between Arg302 and the phenyl ring.

To further rationalize our understanding of the structure−activity relationship (SAR), compounds **2a** and **10a** were docked into the recently published X-ray structure of the NOP receptor (PDB code 4EA3)[13,14] keeping side chains flexible (see Figure 1). In accordance to other aminergic G-protein coupled receptors the central Asp130 plays a major role in the interaction between ligand and receptor. The tertiary amine, which is protonated under physiological conditions, forms an ionic interaction with Asp130. In the case of the trans configured **2a**, cis configuration of both nitrogens, the indole NH forms an additional hydrogen bond with Asp130. This reflects a bidentate, chelating binding mode. In contrast, the cis configured **2b**, trans configuration of both nitrogens, does not allow for the additional hydrogen bond to Asp130, which results in a drop in binding affinity.[15] Additionally the hydrophobic pocket in the binding site of the receptor is occupied by the phenyl moiety of **2a** and **10a**. The hydrophobic pocket formed by the transmembrane helices 4, 5, and 6 (red TMs) is shown on the left side of Figure 1. These two functional groups, a tertiary amine group and the phenyl group at a distinct spatial orientation, form the basic pharmacophore that is present in all examples. It was possible to derive residue ligand interactions from this exercise supporting the observed SAR, although the NOP receptor has been cocrystallized with the antagonist C-24 and the crystal structure therefore reflects the inactive form of the receptor.

The relative spiroether configuration was assigned by 2D NOESY measurements (see Supporting Information).

Uncyclized analogue **29** was finally obtained by building the indole in the last step of the sequence via a Larock cyclization,[16] utilizing 2-iodoaniline and the corresponding triethylsilylalkyne (K_i(*h*NOPr) = 20 nM; K_i(*h*MOPr) = 2 nM).

Functional in vitro investigations of selected examples, using a GTPγS assay, on the NOP and MOP receptors revealed that not all compounds act as full agonists on both receptors (Table 3). Example **12a** appeared to be a partial agonist at the NOP and MOP receptors, while compounds **27a** and **2a** displayed high levels of potency and full efficacy at both the NOP and MOP receptors.

More detailed in vitro characterization revealed that **2a** had a very low potential for disturbing cardiac electrophysiology. By using whole-cell patch-clamp recordings[17] in CHO cells stably transfected with the human ether-à-gogo related gene (hERG), it was demonstrated that up to 30 μM **2a** inhibited the hERG channel by less than 30%. Furthermore, cardiac repolarization measured by conventional microelectrode techniques in isolated guinea-pig papillary muscle[18] was only slightly prolonged. At 10 μM, the action potential duration at 90% repolarization (APD_{90}) was increased by 8 ± 4% (mean ± SD; n = 4) versus time-matched vehicle control. The concentration range at which **2a** may induce a prolongation of cardiac repolarization is thus by a factor of about 10,000× higher than the K_i-values at the NOP and MOP receptors. We therefore consider the risk of ECG changes in vivo very unlikely.

Table 3. Functional Human NOP and MOP Receptor Efficacies

compd	EC_{50} *h*NOPr GTPγS (μM)	rel. eff.[a] hNOPr GTPγS	EC_{50} *h*MOPr GTPγS (μM)	rel. eff.[a] *h*MOPr GTPγS
27a[c]	20	94%	51	104.5%
12a[b]	43	23%	12	70%
2a[d]	11	105%	1	107%

[a]Efficacy of 100% is defined as maximum [^{35}S]GTPγS binding induced by stimulation with nociceptin (NOP receptor) and DAMGO (MOP receptor). [b]Hydrochloride. [c]Dihydrochloride. [d]Citrate.

Cytochrome-P450 inhibition on 1A2, 2C9, 2C19, 2D6, and 3A4 was assessed for **2a** and found to result in IC_{50} values ≥5 μM.

After these promising in vitro results, **2a** was progressed for pharmacokinetic (PK) and efficacy evaluation in rodents. The compound showed poor PK properties in rat with high clearance, large volume of distribution, moderate half-life (Cl = 4.0 L/h·kg; V_{ss} = 7.52 L/kg; $t_{1/2}$ = 1.6 h), and low oral bioavailability (F = 4%; C_{max} = 0.48 nM at a dose of 50 μg/kg). However, because of its high potency, the exposure was considered sufficient to advance it into efficacy profiling.

Compound **2a** was evaluated for its activity in a rat tail-flick model of acute nociceptive pain as well as in a rat spinal nerve ligation (SNL) model of neuropathic pain.

The tail-flick test was carried out in female Sprague−Dawley rats using a modification of the method described by D'Amour and Smith.[19] An increase in tail-flick latency, i.e., the time to withdraw the tail from a radiant heat source, was measured as an indicator of antinociceptive activity of a test compound.[20] Compound **2a** induced dose-dependent antinociception with ED_{50} values (95% CI) of 3.63 (2.95−4.38) nmol/kg i.v. (Figure 2), 19.05 (15.51−23.43) nmol/kg i.p., and 72.93 (59.79−89.35) nmol/kg p.o., and full efficacy at the highest dose tested. A mononeuropathic pain state was induced in male Sprague−Dawley rats by ligation of the left L5/L6 spinal nerves.[21] The antihypersensitive efficacy of compound **2a** was assessed after i.v. and i.p. administration by means of an electronic von Frey filament.[20] Compound **2a** showed a dose-dependent inhibition of mechanical hypersensitivity. Potency was quantified by ED_{50} values (95% CI) of 1.05 (0.79−1.40) nmol/kg i.v. and 4.82 (4.07−5.80) nmol/kg i.p. calculated from the peak effect versus time-matched control values in sham operated animals. A maximum efficacy of 75% was reached after dosing 2.19 nmol/kg i.v. (Figure 3).

Compound **2a** showing antinociceptive as well as anti-hypersensitive efficacy in rats after i.v. dosing with a potency comparable to the strong opioid fentanyl[22] was encouraging and considered proof of concept for our strategy from an

dx.doi.org/10.1021/ml500116x | ACS Med. Chem. Lett. 2014, 5, 851−856

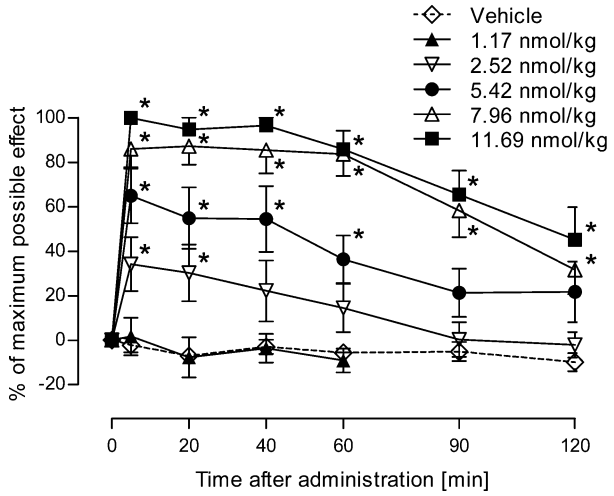

Figure 2. Antinociceptive effect of **2a** citrate after intravenous administration in the rat tail-flick test. Each point of the graph represents the mean ± SEM of the maximum possible effect; $n = 10$ animals per group. *, $p < 0.05$ versus vehicle control.

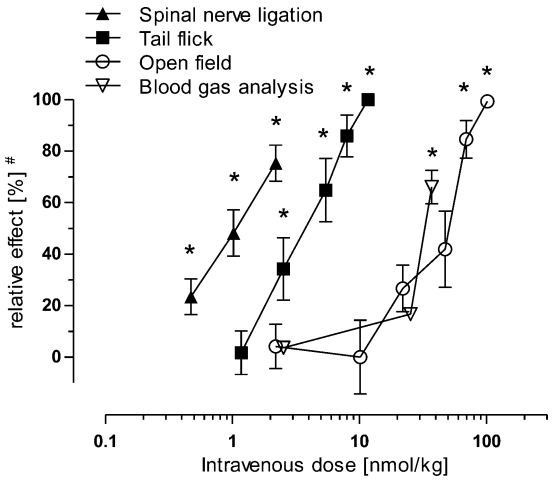

Figure 3. Dose-dependent effects of **2a** citrate on tactile hypersensitivity (spinal nerve ligation), heat nociception (tail-flick), on horizontal distance moved (open field), and on arterial pCO_2 (blood gas analysis) after intravenous administration in rats. #, Relative effect refers to percentage of maximum possible effect (%MPE) for spinal nerve ligation and tail-flick, inhibition of distance moved (open field), and increase in pCO_2 compared to baseline (blood gas analysis). Error bars indicate SEM ($n = 6–10$). *, $p < 0.05$ versus vehicle control.

efficacy point of view. In order to further evaluate whether combined agonistic activity at NOP and MOP receptors also resulted in a broader therapeutic window of these compounds, the side effect profile of **2a** was assessed. Because of the poor PK properties of **2a**, a parenteral route of administration was used to investigate typical MOP receptor mediated side effects like opioid-type sedation, respiratory depression, inhibition of gastrointestinal transit, and induction of physical dependence.

Sedation is a prominent central nervous system (CNS) side effect of MOP receptor agonists resulting in an impairment of spontaneous locomotor activity.[23] A standard open-field test was used to monitor locomotor activity in male Sprague–Dawley rats.[24] After intravenous administration, **2a** dose-dependently reduced the distance that the animals moved within the open-field arena during a 5 min time interval starting 10 min after administration. The ED_{50} value (95% CI) for reduction in distance moved was 42.92 (30.66–62.63) nmol/kg i.v. ($n = 10$/treatment group) (Figure 3).

Potential respiratory depressant activity of **2a** was evaluated in conscious male Sprague–Dawley rats by monitoring arterial blood gas tensions of CO_2 and O_2 (pCO_2 and pO_2). Intravenous administration of **2a** induced a dose-dependent increase in arterial pCO_2 and a concurrent decrease in pO_2. In the highest dose group, treated with 37.04 nmol/kg, pCO_2 was increased by up to 66.1 ± 16.0% (mean ± SD; $n = 6$), while pO_2 was reduced by up to 41.6 ± 3.1% (mean ± SD; $n = 6$) (Figure 3). As a threshold dose for effects of **2a** on respiratory function, an ED_{10} value of 4.28 nmol/kg i.v. ($n = 6$/treatment group) was determined.

The effects of **2a** on gastrointestinal transit were investigated in NMRI mice according to the method of Macht et al.[25] Compound **2a** induced a dose-dependent decrease in intestinal transit with ED_{50} values (mean (95% CI); $n = 10$) of 46.12 (39.56–53.42) nmol/kg i.v. and 143.89 (122.47–170.35) nmol/kg p.o. These doses were 2 to 5 times higher than antinociceptive doses in a mouse tail-flick model, in which ED_{50} values (mean (95% CI); $n = 10$) of 8.87 (7.21–11.26) nmol/kg i.v. and 72.32 (58.97–90.72) nmol/kg p.o. were determined for **2a**.

The potential of **2a** to induce opioid-type physical dependence was investigated by naloxone precipitated withdrawal in NMRI mice.[26] Up to the highest tested dose of 219 nmol/kg i.p. (cumulative dose of 1244 nmol/kg i.p.), **2a** did not induce significant symptoms of withdrawal thereby indicating a very low potential to induce physical dependence (see Supporting Information for figure and details). This dose was at least 5.5 times higher than antinociceptive doses in a mouse tail-flick model, in which an ED_{50} value (mean (95% CI); $n = 10$) of 39.9 (29.3–57.6) nmol/kg i.p. was determined for **2a**.

In summary, spiroether **2a** exhibited strong efficacy in rodent models of acute and neuropathic pain with an about 3 times higher potency in the neuropathic pain model. Moreover, the side effect profile of **2a** reveals clear advantages compared to standard opioids. Morphine, for example, induces marked sedation,[23] as well as respiratory depression, inhibition of gastrointestinal transit, and physical dependence already at doses below or within the half-maximum effective analgesic dose range.[22,27] Compound **2a** exhibits distinct margins of factor 5.5–30 between the ED_{50} in animal models of pain and the doses that induced significant sedation, respiratory depression, or physical dependence. Thus, compounds like **2a** acting as combined NOP and MOP receptor agonists may be particularly suited to provide powerful analgesia with reduced opioid-like side effects and an improved therapeutic index compared to the current standard of care.

On the basis of these overall very promising proof of concept results for **2a** we continued to investigate the structural class of the spiroethers in more depth, especially aiming at improving the PK parameters.

■ ASSOCIATED CONTENT

Supporting Information

Assay description and experimental procedures for the synthesis and characterization of selected compounds. This material is available free of charge via the Internet at http://pubs.acs.org.

dx.doi.org/10.1021/ml500116x | ACS Med. Chem. Lett. 2014, 5, 851–856

AUTHOR INFORMATION

Corresponding Author

*(S.S.) E-mail: stefan.schunk@grunenthal.com.

Notes

The authors declare no competing financial interest.

ACKNOWLEDGMENTS

We thank H. Steinhagen, P. Ratcliffe, S. Frosch, and E. Hoppe for very helpful discussions, F. Theil (ASCA GmbH) for conception and realization of compounds, T. Koch for obtaining NOP and MOP receptor binding data, J. Glembin for carrying out the electrophysiology in the papillary muscle model, and S. Brenner, P. Günther, B. Liebenhoff, M. Mülfarth, H .J. Weber, and R. Woloszczak for technical assistance with the in vivo experiments. Detailed 2D NMR analysis for determination of stereochemical configuration by O. Aulenbacher, P. Jonas, and M. Schade, high-resolution mass by J. Bergstreiser and M. Fuhr, and eADME characterization by S. Steufmehl are greatly acknowledged.

ABBREVIATIONS

CHO, Chinese hamster ovary cells; CI, confidence interval; CNS, central nervous system; DOP, delta opioid peptide; EC_{50}, concentration with half-maximum inducible [^{35}S]GTPγS binding; ED_{50}, half-maximum effective dose; E_{max}, maximum possible effect for the agonist; GTPγS, guanosine-5′-[γ-thio]triphosphate; *h*NOPr, Human nociceptin/orphanin FQ receptor; *h*MOPr, Human μ opioid peptide receptor; HCl, hydrochloride; IC_{50}, half-maximum inhibitory concentration; i.v., intravenous; K_i, dissociation constant for inhibitor binding; KOP, kappa opioid peptide; MOP, mu opioid peptide; MPE, maximum possible effect; NOP, nociceptin/orphanin FQ peptide; r, receptor; SNL, spinal nerve ligation

REFERENCES

(1) Zöllner, C.; Stein, C. Opioids. *Handb. Exp. Pharmacol.* **2007**, 31−63.

(2) Meunier, J. C.; Mollereau, C.; Toll, L.; Suaudeau, C.; Moisand, C.; Alvinerie, P.; Butour, J.-L.; Guillemot, J.-C.; Ferrara, P.; Monsarrat, B.; Mazargull, H.; Vassart, G.; Parmentier, M.; Costentin, J. Isolation and structure of the endogenous agonist of opioid receptor-like ORL1 receptor. *Nature* **1995**, *377*, 532−535.

(3) Reinscheid, R. K.; Nothacker, H. P.; Bourson, A.; Ardati, A.; Henningsen, R. A.; Bunzow, J. R.; Grandy, D. K.; Langen, H.; Monsma, F. J.; Civelli, O. Orphanin FQ: A neuropeptide that activates an opioidlike G protein-coupled receptor. *Science* **1995**, *270*, 792−794.

(4) Cox, B. M.; Borsodi, A.; Calo, G.; Chavkin, C.; Christie, M. J.; Civelli, O.; Devi, L. A.; Evans, C.; Hollt, V.; Henderson, G.; Kieffer, B.; Kitchen, I.; Kreek, M. J.; Liu Chen, L. Y.; Meunier, J. C.; Portoghese, P. S.; Shippenberg, T. S.; Simon, E. J.; Toll, L.; Traynor, J. R.; Ueda, H. Wong, Y. H. Opioid Receptors: Introduction. http://www.iuphar-db.org/DATABASE/FamilyIntroductionForward?familyId=50.

(5) Cremeans, C. M.; Gruley, E.; Kyle, D. J.; Ko, M.-C. Roles of μ-opioid receptors and nociceptin/orphanin FQ peptide receptors in buprenorphine-induced physiological responses in primates. *J. Pharmacol. Exp. Ther.* **2012**, *343*, 72−81.

(6) Toll, L. The use of bifunctional NOP/Mu and NOP receptor selective compounds for the treatment of pain, drug abuse, and psychiatric disorders. *Curr. Pharm. Des.* **2013**, *19*, 7451−60.

(7) Lednicer, D.; Von Voigtlander, P. F.; Emmert, D. E. 4-Amino-4-arylcyclohexanones and their derivates, a novel class of analgesics. 1. Modification of the aryl ring. *J. Med. Chem.* **1980**, *23*, 424−425.

(8) Lednicer, D.; Von Voigtlander, P. F.; Emmert, D. E. 4-Aryl-4-aminocyclohexanonesa and their derivatives, a novel class of analgesics. 3. *m*-Hydroxyphenyl derivatives. *J. Med. Chem.* **1981**, *24*, 341−346.

(9) Lednicer, D.; Von Voigtlander, P. F.; Emmert, D. E. 4-Amino-4-arylcyclohexanones and their derivatives: a novel class of analgesics. 2. Modification of the carbonyl function. *J. Med. Chem.* **1981**, *24*, 404−408.

(10) Hatakeyama, S.; Mori, H.; Kitano, K.; Yamada, H.; Nishizawa, M. Efficient reductive etherification of carbonyl compounds with alkoxytrimethylsilanes. *Tetrahedron Lett.* **1994**, *35*, 4367−4370.

(11) Von Voigtlander, P. F.; Lednicer, D.; Lewis, R. A. 4-Aryl-4-aminocyclohexanone derivatives: A chemically novel series of analgesiscs including opioid antagonists and extremely potent agonists. *Proc. Int. Narc. Res. Club Conf.* **1980**, 17−21.

(12) Larghi, L. E.; Kaufman, T. S. The oxa-Pictet−Spengler cyclization: Synthesis of isochromans and related pyran-type heterocycles. *Synthesis* **2006**, *2*, 187−220.

(13) Thompson, A. A.; Liu, W.; Chun, E.; Katritch, V.; Wu, H.; Vardy, E.; Huang, X.-P.; Trapella, C.; Guerrini, R.; Calo, G.; Roth, B. L.; Cherezov, V.; Stevens, R. C. Structure of the nociceptin/orphanin FQ receptor in complex with a peptide mimetic. *Nature* **2012**, *485*, 395−399.

(14) Standard modeling techniques have been applied to dock, optimize, and visualize the binding modes of our compounds as implemented in MOE2012.10 (Molecular Operating Environment 2012, CCG, Montreal, Canada).

(15) For 2D interaction plot, see Supporting Information.

(16) Larock, R. C.; Yum, E. K. Synthesis of indoles via palladium-catalyzed heteroannulation of internal alkynes. *J. Am. Chem. Soc.* **1991**, *113*, 6689−6690.

(17) Hamill, O. P.; Marty, A.; Neher, E.; Sakmann, B.; Sigworth, F. J. Improved patch-clamp techniques for high-resolution current recording from cells and cell-free membrane patches. *Pflugers Arch.* **1981**, *391*, 85−100.

(18) Gjini, V.; Schreieck, J.; Korth, M.; Weyerbrock, S.; Schömig, A.; Schmitt, C. Frequency dependence in the action of the class III antiarrhythmic drug dofetilide is modulated by altering L-type calcium current and digitalis glucoside. *J. Cardiovasc. Pharmacol.* **1998**, *31*, 95−100.

(19) D'Amour, F. E.; Smith, D. L. A method for determining loss of pain sensation. *J. Pharmacol. Exp. Ther.* **1941**, *72*, 74−79.

(20) Tzschentke, T. M.; Christoph, T.; Kögel, B.; Schiene, K.; Hennies, H.-H.; Englberger, W.; Haurand, M.; Jahnel, U.; Cremers, T. I. F. H.; Friderichs, E.; de Vry, J. (−)-(1*R*,2*R*)-3-(3-Dimethylamino-1-ethyl-2-methyl-propyl)-phenol hydrochloride (Tapentadol HCl): a novel μ-opioid receptor agonist/norepinephrine reuptake inhibitor with broad-spectrum analgesic properties. *J. Pharmacol. Exp. Ther.* **2007**, *323*, 265−276.

(21) Kim, S. H.; Chung, J. M. An experimental model for peripheral neuropathy produced by segmental spinal nerve ligation in the rat. *Pain* **1992**, *50*, 355−363.

(22) Meert, T. F.; Vermeirsch, H. A. A preclinical comparison between different opioids: antinociceptive versus adverse effects. *Pharmacol., Biochem. Behav.* **2005**, *80*, 309−326.

(23) Winter, L.; Nadeson, R.; Tucker, A.; Goodchild, C. S. Antinociceptive properties of neurosteroids: a comparison of alphadolone and alphaxalone in potentiation of opioid antinociception. *Anesth. Analg.* **2003**, *97*, 798−805.

(24) Ericson, E.; Samuelsson, J.; Ahlenius, S. Photocell measurements of rat motor activity: a contribution to sensitivity and variation in behavioral observations. *J. Pharmacol. Methods* **1991**, *25*, 111−122.

(25) Macht, D. I.; Barba-Gose, J. Two new methods for the pharmacological comparison of insoluble purgatives. *J. Am. Pharm. Assoc.* **1931**, *20*, 558−564.

(26) Saelens, J. K.; Garant, F. R.; Sawyer, W. K. The mouse jumping test: a simple screening method to estimate the physical dependence capacity of analgesics. *Arch. Int. Pharmacodyn.* **1971**, *190*, 213−218.

(27) Tzschentke, T. M.; de Vry, J.; Terlinden, R.; Hennies, H.-H.; Lange, C.; Strassburger, W.; Haurand, M.; Kolb, J.; Schneider, J.; Buschmann, H.; Finkam, M.; Jahnel, U.; Friderichs, E. Tapentadol hydrochloride. Analgesic, mu-opioid receptor agonist, noradrenaline reuptake inhibitor. *Drugs Future* **2006**, *31*, 1053−1061.